

2009

# Development of novel nanostructured conducting polypyrrole fibres

Javad Foroughi

*University of Wollongong*, foroughi@uow.edu.au

## UNIVERSITY OF WOLLONGONG

### COPYRIGHT WARNING

You may print or download ONE copy of this document for the purpose of your own research or study. The University does not authorise you to copy, communicate or otherwise make available electronically to any other person any copyright material contained on this site. You are reminded of the following:

This work is copyright. Apart from any use permitted under the Copyright Act 1968, no part of this work may be reproduced by any process, nor may any other exclusive right be exercised, without the permission of the author.

Copyright owners are entitled to take legal action against persons who infringe their copyright. A reproduction of material that is protected by copyright may be a copyright infringement. A court may impose penalties and award damages in relation to offences and infringements relating to copyright material. Higher penalties may apply, and higher damages may be awarded, for offences and infringements involving the conversion of material into digital or electronic form.

**Unless otherwise indicated, the views expressed in this thesis are those of the author and do not necessarily represent the views of the University of Wollongong.**

## Recommended Citation

Foroughi, Javad, Development of novel nanostructured conducting polypyrrole fibres, Doctor of Philosophy thesis, Intelligent Polymer Research Institute, Faculty of Engineering, University of Wollongong, 2009. <https://ro.uow.edu.au/theses/3073>

Research Online is the open access institutional repository for the University of Wollongong. For further information contact the UOW Library: [research-pubs@uow.edu.au](mailto:research-pubs@uow.edu.au)

## **NOTE**

This online version of the thesis may have different page formatting and pagination from the paper copy held in the University of Wollongong Library.

## **UNIVERSITY OF WOLLONGONG**

### **COPYRIGHT WARNING**

You may print or download ONE copy of this document for the purpose of your own research or study. The University does not authorise you to copy, communicate or otherwise make available electronically to any other person any copyright material contained on this site. You are reminded of the following:

Copyright owners are entitled to take legal action against persons who infringe their copyright. A reproduction of material that is protected by copyright may be a copyright infringement. A court may impose penalties and award damages in relation to offences and infringements relating to copyright material. Higher penalties may apply, and higher damages may be awarded, for offences and infringements involving the conversion of material into digital or electronic form.

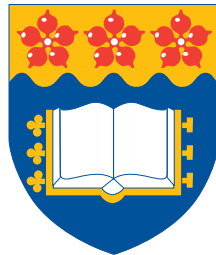
# **Development of Novel Nanostructured Conducting Polypyrrole Fibres**

A thesis submitted in fulfilment of the  
requirements for the award of the degree

DOCTOR OF PHILOSOPHY

From

UNIVERSITY OF WOLLONGONG



by

JAVAD FOROUGHI

(BSc & MSc Textile Engineering)

Intelligent Polymer Research Institute

Faculty of Engineering

September 2009

*To my parents for their endless love.*

*To my country IRAN*

# CERTIFICATION

I, *Javad Foroughi*, declare that this thesis, submitted in fulfilment of the requirements for the award of *Doctor of Philosophy*, in the *Faculty of Engineering*, University of Wollongong, is wholly my own work unless otherwise referenced or acknowledged. The document has not been submitted for qualifications at any other academic institution.

Javad Foroughi

September 2009

## ACKNOWLEDGEMENTS

I would like to thank my supervisors Prof. Gordon Wallace and Prof. Geoff Spinks for supervision throughout this work. Their guidance and support throughout the course of this project will not be forgotten in my life.

I greatly appreciate to Prof. Leon Kane-Maguire for his guidance, advice and for his careful proof reading and help on the first draft of this thesis.

I would also like to thank Prof. Ray Baughman and Dr. Mikhail Kozlov from Nanotech Institute, University of Texas at Dallas. Also the Australian Research Network for Advanced Materials (ARNAM) for financial support for this visit.

My colleagues and friends at Intelligent Polymer Research have offered help and support over the past 3 years that I have been a part of that group. In particular, I would like to thank Dr. Philip Whitten, Prof. Chee O Too, Prof. Peter Innis, Dr. Joe Razal, Dr. Jun Chen, Dr. Jakub Mazurkiewicz, Dr. Scott McGovern, Adrian Gestos, Dr. Johana Mbere, and Dr. Grant Mathieson for their unforgotten help in the laboratory. I would like to thank Prof. Rian Dippenaar for his support during my study.

The financial support provided by the Australian Research Council in the form of an Australian Postgraduate Award and by Prof. Gordon Wallace for my PhD scholarship is gratefully acknowledged.

Finally I am grateful to my family in IRAN who has provided continued support throughout this study and indeed for my entire life.

# PUBLICATIONS

## **Journal:**

1-Javad Foroughi, G. Spinks, G. Wallace,” A Reactive Wet Spinning Approach to Polypyrrole Fibres”, to be submitted.

2- Javad Foroughi, G. Spinks, G. Wallace,” Effect of Synthesis Conditions on the Properties of Wet Spun Polypyrrole Fibres”, Synthetic Metals, 2009 159(17-18): p. 1837-1843

3-Javad Foroughi, G. Spinks, P. Whitten, G. Wallace,” Production of polypyrrole fibres through a wet spinning process”, Synthetic Metals, 2008 158(3-4): p. 104-107

## **Conferences:**

1- Javad Foroughi, Geoffrey M. Spinks and Gordon G. Wallace, “ A Novel Approach to Produce Polypyrrole Biopolymer Nano-Composite Fibres”, Electromaterials Symposium 2009(ACES) “ Nanostructured Electromaterials”, Australia, 4-6 Feb. 2009.

2- Javad Foroughi, Geoffrey M. Spinks and Gordon G. Wallace, “A comparison of chemically prepared and electrochemically prepared polypyrrole films and fibres for artificial muscles”, The NanotxUSA’08, International Nanotechnology conference and trade Expo, Dallas, Texas, USA 2-3 October 2008.

3- Javad Foroughi, Geoffrey M. Spinks, Xiao Liu and Gordon G. Wallace, “Towards to Development of NanoBionics Using Polypyrrole-Biopolymer Fibres”, Asia Pacific symposium on Nano Bionics, Australia, 22-25 June 2008.

4- Gordon G. Wallace, Javad Foroughi, Charles Mire, Marc in het Panhuis and Geoffrey Spinks, “Fiber Spinning and Ink Jet Printing New Advances in Conducting Polymer Device Fabrication” ,15th International symposium on smart structures and materials & nondestructive evaluation and health monitoring, San Diego, California USA 9-13 March 2008.

5- Javad Foroughi, Geoffrey M. Spinks, Philip G. Whitten and Gordon G. Wallace, "A Novel Approach to Produce Nano-Composite Polypyrrole-Carbon Nanotube Fibres", International Conference on Nanoscience and Nanotechnology, Melbourne, Australia, 25-29 Feb. 2008.

6- Javad Foroughi, Geoffrey M. Spinks, Philip G. Whitten and Gordon G. Wallace, "Highly flexible and conducting electropolymerized polypyrrole film", 3rd International Electromaterials Science Symposium (Advanced materials for energy storage and generation), Monash University, Australia, 21-22Feb 2008.

7- Javad Foroughi, Geoffrey M. Spinks, Philip G. Whitten and Gordon G. Wallace, "A new opportunity for conducting polymers using polypyrrole fibres", 3rd International Electromaterials Science Symposium (Advanced materials for energy storage and generation), Monash University, Australia, 21-22Feb 2008.

8- Javad Foroughi, G. Spinks, C. Lynam, P. Whitten, G. Wallace, "The development of Polypyrrole single walled carbon nanotube composite fibres through wet spinning process", 2nd International Symposium on Electromaterials Science, Australia, 7-8 Feb 2007.

9- Javad Foroughi, G. Spinks, G. Wallace, "How artificial muscles can be improved using polypyrrole", ARNAM Annual 2008 workshop, Deakin University, Victoria, 15-18 Dec. 2008.

10- Javad Foroughi, G. Spinks, G. Wallace, "First ever production of polypyrrole fibres", HDR Conference, University of Wollongong, 26 Sep. 2007.

11- Javad Foroughi, G. Spinks, C. Lynam, P. Whitten, G. Wallace, "Novel composite Polypyrrole CNT fibres through wet spinning process", 6th National Iranian Textile Engineering Conference, 8-9 May 2007.

12- Javad Foroughi, G. Spinks, G. Wallace, "Development of e-Textiles using conducting polymers", HDR Conference, University of Wollongong, Sep. 2006.



**Manuscript in preparation:**

1-Javad Foroughi, G. Spinks, G. Wallace,” A novel DEHS doped Polypyrrole”, Manuscript in preparation, 2009.

2-Javad Foroughi, G. Spinks, G. Wallace,” A New Opportunity for Bionics Using DEHS Doped Polypyrrole”, Manuscript in preparation, 2009.

## **Abstract:**

Polypyrrole (PPy) as a conducting polymer has potential applications in electrical and electronic devices because of its high electrical conductivity, environmental stability and redox activity. There have been many attempts to endow electrically PPy with processibility. Although some success has been achieved *via* synthesising soluble PPy, there have remained difficulties to fabricate this material through fibre spinning due to its low molecular weight and poor mechanical properties. Prior to this thesis, there was no report of the production of PPy fibres. This project therefore aimed to produce novel “*polypyrrole fibres via the development of nanostructured conducting polypyrrole*” by fibre spinning of PPy and to investigate the formed fibres for applications such as actuators, e-textiles, batteries, sensors and biomedical areas.

As a result of the research conducted for this thesis, polypyrrole fibres have been produced for the first time. The initial wet-spinning process was enabled by the use of highly soluble non-functionalised PPy using di-(2-ethylhexyl)sulfosuccinate (DEHS) dopant, and the generation of a spinning solution of the PPy-DEHS in dichloroacetic acid (DCAA) solvent. Subsequent work sought to improve the properties of these first generation PPy-DEHS fibres by increasing the molecular weight, addition of carbon nanotubes (CNTs) and addition of a supporting polymer (alginate). The use of the host polymer also enabled a new fibre spinning method to be developed that included an *in situ* polymerization process. Carbon nanotubes additions were achieved in two ways: firstly by adding small amounts of CNTs to the spinning dope; and secondly, a completely novel approach was developed whereby PPy was polymerized onto and into a CNT yarn.

Each of the methods used to generate PPy fibres gave different performances in terms of mechanical strength / stiffness; electrical conductivity and electroactivity. Generally, it was found that adding of carbon nanotubes to the PPy improved the strength, stiffness and conductivity. The highest conductivity and Young's modulus of any conducting polymer based fibre reported to date was obtained by incorporating PPy into a CNT yarn. The more robust fibres were assessed as mechanical actuators and a maximum strain of 2.5% was produced from the high molecular weight PPy-DEHS fibre.

In summary, a range of novel fibrous PPy materials have been developed for possible use in applications such as actuators, sensors, artificial muscles, batteries and biomedical applications. The main aim of the thesis was to develop methods for continuous production of doped PPy fibres. This aim was successfully completed with a variety of different fibre compositions and properties demonstrated using a range of different fibre processing methods.

# ABBREVIATIONS

A	Ampere
A <sup>-</sup>	Anion
AC	Alternating current
ACN	Acetonitrile
Ag/Ag <sup>+</sup>	Silver/silver ion reference electrode
Ag/AgCl	Silver/silver chloride reference electrode
BMI.BF <sub>4</sub>	1-Butyl-3-methyl-imidazolium tetrafluoroborate
C	Coulomb
cm	Centimetre
conc.	Concentration
CV	Cyclic voltammetry
D	Diffusion coefficient
DBS-	Dodecylbenzene sulfonate
e <sup>-</sup>	Electron
E	Potential
E <sub>app</sub>	Applied potential
E <sub>C</sub>	Electrochemical/Electrochemistry
E <sub>f</sub>	Final potential
E <sub>i</sub>	Initial potential
E'	Loss modulus
E''	Storage modulus
F	Faraday constant
g	Gram
i	Current
L	Litre
M	Molar
mA	Milliampere
min	Minute
ml	Millilitre
mV	Millivolt
MWNT	multi wall carbon nanotubes

n	Number of electrons
NIR	Near infra red
NMP	N-methyl pyrrolidinone
PAni	Polyaniline
PC	Propylene carbonate
PF <sub>6</sub> -	Hexafluorophosphate
PPy	Polypyrrole
PPy/Cl	Polypyrrole chloride
PPy/ClO <sub>4</sub>	Polypyrrole perchlorate
PPy/NO <sub>3</sub>	Polypyrrole nitrate
PPy/DBS	Polypyrrole Dodecylbenzenesulfonate
PPy/PF <sub>6</sub>	Polypyrrole hexafluorophosphate
PPy/pTS	Polypyrrole p-toluene sulphonate
Psi	Pound per square inch
PTh	Polythiophene
PVA	Polyvinyl alcohol
Pt	Platinum
<i>p</i> TS.Na	p-toluene sulphonic acid sodium salt
Q	Charge
R	Resistance (ohm)
s	Second
S	Siemens
SEM	Scanning electron microscopy
SWNT	Single wall carbon nanotubes
S/N	Sulphur to nitrogen atomic ratio
t	Time
T	Temperature
TEM	Transmission electron microscopy
T <sub>g</sub>	Glass transition temperature
TGA	Thermogravimetric analysis
TM	Tangential mode (G band)
TPa	Tera pascal
TBA.PF <sub>6</sub>	Tetrabutylammonium hexafluorophosphate
TFSI-	(bis) trifluoromethanesulfonimide

V	Volt
$V_d$	Drawing velocity (m/min)
$V_i$	Injection rate (g/min)
$V_t$	Take up velocity (m/min)
$\mu$	Micro (prefix)
$\nu$	Scan rate
$\gamma$	Shear rate (s <sup>-1</sup> )
$\eta$	Viscosity (mPa.s = cP)
$\rho$	Density (g/cm <sup>3</sup> )
$\sigma$	Conductivity (S/cm)
$X^+$	Cation

# LIST OF FIGURES AND TABLES

## Chapter 1

Figure 1.1:	3
Chemical structures of selected $\pi$ -conjugated inherently conducting polymers in their neutral undoped form.	
Figure 1.2:	5
Schematic showing the formation of polaron and bipolaron states in PPy.	
Figure 1.3:	7
A general scheme for polymerisation of aniline.	
Figure 1.4:	8
Different states of oxidation in the base form of PANi.	
Figure 1.5:	12
Schematic electronic energy level diagrams for (a) neutral, (b) polaronic, (c) bipolaronic, and (d) fully doped polypyrrole.	
Figure 1.6:	13
Polymerisation mechanism for pyrrole through the coupling of two radical cations.	
Figure 1.7:	18
Structure of p-dodecylbenzenesulphonic acid (DBSA).	
Figure 1.8:	20
Structure of di(2-ethylhexyl) sulfosuccinate sodium salt (NaDEHS).	
Figure 1.9:	24
Phase diagram of a ternary system consisting of polymer, solvent and non-solvent.	
Figure 1.10:	25
Schematic showing the set up used for wet-spinning of fibres.	

## Chapter 2

Figure 2.1:	40
Light scattering and backscatter detection of the sample.	
Figure 2.2:	42
Correlation of different particle sizes.	
Figure 2.3:	42

Differences between particle size distribution presented by: ( a) Number, (b) Volume, and (c) Intensity.

Figure 2.4: 52

A typical cyclic voltammogram showing an oxidation peak at E<sub>pa</sub> with a maximum anodic current (i<sub>pa</sub>) in the forward scan, and a corresponding reduction peak at E<sub>pc</sub> with a maximum cathodic current (i<sub>pc</sub>) in the reverse scan.

### Chapter 3

Figure 3.1: 62

Schematic diagram of spinning apparatus.

Figure 3.2: 64

UV-Vis/NIR spectra of dilute solutions (0.01% w/w) of PPy-DEHS in various solvents (DCAA, DMF, DMPU).

Figure 3.3: 65

Particle size distribution obtained by light scattering of dilute solutions (0.01 % w/w) of PPy-DEHS in various solvents.

Figure 3.4: 66

Schematic diagram of spinning apparatus (a) and photograph of a resulting PPy-DEHS fibre (b).

Figure 3.5: 67

SEM micrographs of PPy-DEHS fibre at low (a,c) and higher (b,d) magnification, showing the fibre cross-section (a,b) and surface (c,d).

Figure 3.6: 68

Stress-strain curves obtained from tensile testing of three PPy-DEHS fibres prepared and tested under identical conditions.

Figure 3.7: 70

Cyclic voltammogram of PPy-DEHS fibre in aqueous 1.0 M NaNO<sub>3</sub>. Potential was scanned between -0.9V and +0.4V (vs. Ag/AgCl) at 100 mVs<sup>-1</sup>.

### Chapter 4

Figure 4.1: 80

TEM images of PPy-CNT from a dried DCAA dispersion.

Figure 4.2: 81



Size distribution of a dilute solution (0.04% w/v) of PPy-DEHS/CNT and CNTs in DCAA (freshly prepared and after 72 hr).

Figure 4.3: **82**

UV-Vis/NIR spectra of PPy-DEHS/CNT composite and of PPy-DEHS (0.01% w/v) in DCAA.

Figure 4.4: **84**

SEM of PPy-DEHS/CNT fibre: (a) surface morphology, and (b) cross-section.

Figure 4.5: **85**

SEM of PPy-DEHS/CNT fibre: (a, c, e) water, and (b, d, f) NH<sub>4</sub>OH (10% v/v) in water as spinning coagulation bath.

Figure 4.6: **86**

Raman spectra for: PPy-DEHS/CNT fibre, PPy-DEHS fibre and CNT powder.

Figure 4.7: **87**

Cyclic voltammogram of the PPy-DEHS/CNT fibre. Potential was scanned between -0.9 and +0.7 V (vs. Ag/AgCl) in 1.0 M NaNO<sub>3</sub> (aq) at 100 mVs<sup>-1</sup>.

Figure 4.8: **89**

Stress-strain curves obtained for PPy-DEHS and the PPy-DEHS/CNT nanocomposite fibre.

Figure 4.9: **90**

TGA thermograms of DEHS, PPy-DEHS, PPy-DEHS/CNT fibres and pristine CNT.

Figure 4.10: **93**

Effect of co-solvent on solubility of PPy-DEHS polymerization at 0°C in the present of; (a), ethanol (20% v/v), (b), ethanol (25% v/v), (c), ethanol (35% v/v).

Figure 4.11: **94**

TGA thermograms of PPy-DEHS powders prepared at 0°C with (a) no ethanol, and (b) 35% (v/v) ethanol in the aqueous polymerization solution (i.e. samples 1 and 7).

The TGA for the DEHS dopant is also shown.

Figure 4.12: **96**

Specific viscosity of low temperature polymerized PPy-DEHS in DCAA solvent as a function of polymer concentration. Inset shows a wider concentration range.

Figure 4.13: **97**

Reduced viscosity of low temperature and standard PPy-DEHS in DCAA solvent as a function of polymer concentration.

Figure 4.14: **98**

Size distribution obtained by light scattering of a dilute solution (0.01 % w/w) of high molecular weight PPy-DEHS and standard PPy-DEHS in DCAA.

Figure 4.15: **99**

UV-Vis/NIR spectrum of a dilute solution (0.01% w/w) of high molecular weight PPy-DEHS in DCAA solvent.

Figure 4.16: **101**

FTIR spectra of high molecular weight and standard PPy-DEHS powders.

Figure 4.17: **102**

TGA thermograms for high molecular weight and standard PPy-DEHS powder, for PPy without DEHS, and for dopant DEHS.

Figure 4.18: **103**

X-ray diffraction patterns of high molecular weight and standard PPy-DEHS powders.

Figure 4.19: **106**

The viscosity of spinning solutions (18% w/w) of high molecular weight and standard PPy-DEHS dissolved in DCAA, as a function of shear rate.

Figures 4.20: **107**

SEM micrographs of high molecular weight PPy-DEHS fibres at low and higher magnification, showing the fibre cross-section (d, f, h) and surface (b, e, g).

Figure 4.21: **109**

Storage modulus of undrawn high molecular weight PPy-DEHS fibre and tan delta ( $\delta = E''/E'$ , where  $E''$  = storage modulus,  $E'$  = loss modulus) of undrawn PPy fibre vs. temperature.

Figure 4.22: **109**

Stress-strain curve during stretching (drawing) at  $\sim 100^\circ\text{C}$  for high molecular weight PPy-DEHS fibre.

Figure 4.23: **111**

Stress-strain curves obtained from tensile testing of various PPy-DEHS fibres.

Figure 4.24: **112**

Cyclic voltammograms of drawn high molecular weight PPy-DEHS fibre. Potential was scanned between -0.9 V and +0.6 V (vs. Ag/AgCl) in 0.10 M DEHS in acetonitrile/water (1:1) at  $100 \text{ mVs}^{-1}$ .

## Chapter 5

- Figure 5.1: **121**  
UV-Vis/NIR spectra of chemically (Chem) and electrochemically (Elect) prepared PPy-DEHS films.
- Figure 5.2: **123**  
TGA of electropolymerized PPy-DEHS film, chemically polymerized PPy-DEHS powder, cast PPy-DEHS film, and DEHS dopant.
- Figure 5.3a: **124**  
Raman spectra of an electropolymerized PPy-DEHS film.
- Figure 5.3b: **125**  
Raman spectra of chemically polymerized PPy-DEHS powder and cast PPy-DEHS film.
- Figure 5.4: **128**  
FTIR spectra of a electropolymerized PPy-DEHS film, compared with chemically polymerized PPy-DEHS powder and a film.
- Figure 5.5: **130**  
SEM micrographs of PPy-DEHS at low magnification: electrochemical (a,b), cast film(e,f); and at higher magnification: electrochemical (c,d), cast film(g), powder(h).
- Figure 5.6: **132**  
Stress-strain curves obtained for two chemically prepared PPy cast films.
- Figure 5.7: **132**  
Stress-strain curves obtained from tensile testing of two electrochemically prepared PPy films.
- Figure 5.8: **134**  
Cyclic voltammogram of electrochemically polymerized PPy-DEHS film. Potential was scanned between -0.9V and +0.7V (vs. Ag/AgCl) in 0.10 M DEHS in acetonitrile /water (1:1) at 100 m Vs<sup>-1</sup>.
- Figure 5.9: **135**  
Cyclic voltammogram of chemically polymerized PPy-DEHS film. Potential was scanned between -0.9V and +0.7V (vs. Ag/AgCl) in 0.10 M DEHS in acetonitrile /water (1:1) at 100 m Vs<sup>-1</sup>.
- Figure 5.10: **136**

Cyclic voltammogram of chemically polymerized PPy-DEHS fibre. Potential was scanned between -0.9V and +0.4V (vs. Ag/AgCl) in 1 M NaNO<sub>3</sub> at 100 m Vs<sup>-1</sup>.

Figurer 5.11: **137**

Electrochemical actuation of electropolymerized PPy-DEHS film. Potential was scanned between -0.9V and +0.8V (vs. Ag/AgCl) in 0.10 M DEHS in acetonitrile /water (1:1) at 1 m Vs<sup>-1</sup>.

Figurer 5.12: **138**

Electrochemical actuation of chemically polymerized PPy-DEHA (cast film). Potential was scanned between -0.9V and +0.8V (vs. Ag/AgCl) in 0.10 M DEHS in acetonitrile /water (1:1) at 1 m Vs<sup>-1</sup>.

## **Chapter 6**

Figure 6.1: **147**

Continuous wet-spinning line for production of PPy-Alg bicomponent fibres.

Figure 6.2: **148**

Continuous wet-spinning and polymerization line.

Figure 6.3: **149**

Size distribution of a dilute dispersion (0.04% w/v) of PPy-DEHS-DBSA and of a dilute spinning solution (0.04% w/v) of PPy-DEHS-DBSA/Alginate in water.

Figure 6.4: **150**

Variation in viscosity of PPy-alginate spinning solution at different shear rates.

Figure 6.5: **151**

UV-Vis/NIR spectra of aqueous PPy-Alg spinning solution (0.01% w/v).

Figure 6.6: **152**

SEM of PPy-Alg bicomponent fibre: (a,b) cross-section and (c) surface morphology.

Figure 6.7: **153**

Stress-strain curves obtained for two PPy-Alginate bicomponent fibres.

Figure 6.8: **155**

Variation in viscosity at different shear rates of spinning solutions of alginate and alginate - pyrrole with and without CNTs at different shear rates.

Figure 6.9: **156**

UV-Vis/NIR spectra of as-spun Alginate - pyrrole fibre. Time = 0 is the point at which the alginate-pyrrole fibre enters the oxidation bath from the drawing zone (see

Fig. 6.2). Time = 45 is 45 min after the fibre had first contact with the coagulation bath.

Figure 6.10: **157**

UV-Vis/NIR spectra of as-spun PPy-Alg-CNT fibres obtained using different oxidant/dopant systems.

Figure 6.11: **158**

SEM micrographs of the surface of (a) Alginate; PPy-(APS/DEHS)-Alg; (b-c) low and (d) higher magnification, PPy-(APS/DEHS)-Alg-CNT; (e) low and (f) higher magnification.

Figure 6.12: **159**

SEM micrographs at low magnification of the PPy-Alg-CNT fibres with different oxidant/dopant; (a) APS/*p*TS (b) FeCl<sub>3</sub>/DEHS; (c) FeCl<sub>3</sub>/*p*TS.

Figure 6.13: **160**

SEM micrographs at high magnification of surface of the as-spun PPy-Alg-CNT fibres with different oxidant/dopant; (a-b) APS/*p*TS; (c-d) FeCl<sub>3</sub>/DEHS; (e-f) FeCl<sub>3</sub>/*p*TS.

Figure 6.14: **163**

Raman spectra of novel PPy-Alg-CNT (APS/DEHS) nanocomposite fibre, PPy fibre and single-walled CNTs as labelled.

Figure 6.15: **164**

Map of the cross-section of bicomponent PPy-Alg fibre.

Figure 6.16: **164**

Map of the surface of bicomponent PPy-Alg fibre.

Figure 6.17: **165**

The averaged Raman spectra from cross-section and surface of PPy-Alg bicomponent fibre.

Figure 6.18: **166**

Stress-strain curves obtained from tensile tests of Alginate fibre, PPy-Alg and PPy-Alg-CNT composite fibres. APS/DEHS was used as oxidant /dopant for the pyrrole polymerisation in each case.

Figure 6.19: **167**

Stress-strain curves obtained from tensile tests of PPy-Alg-CNT nanocomposite fibres with different oxidant/dopant systems.

Figure 6.20: **169**

Cyclic voltammograms of PPy-Alg and PPy-Alg-CNT (APS/DEHS) fibres. Potential was scanned between -0.7 and +0.7V (vs. Ag/AgCl) in 1.0 M NaNO<sub>3</sub> at 100 mVs<sup>-1</sup>.

Figure 6.21: **170**

Cyclic voltammograms of PPy-Alg-CNT fibres prepared with different oxidant/dopant systems. Potential was scanned between -0.7 and +0.7V (vs. Ag/AgCl) in 1.0 M NaNO<sub>3</sub> at 100 mVs<sup>-1</sup>.

Figure 6.23: **171**

Cyclic voltammograms of PPy-Alg-CNT (APS/DEHS) fibre. Potential was scanned between -0.9V and +0.7V (vs. Ag/AgCl) in 0.1 M DEHS in acetonitrile/water (1:1) at 100 mVs<sup>-1</sup>.

## **Chapter 7**

Figure 7.1: **179**

Spinning of CNT yarn from multi walled carbon nanotube forest.

Figure 7.2: **181**

Preparation of PPy/CNT yarn using vapour phase polymerization; (a) pristine CNT yarn (b) CNT yarn into oxidant/dopant solution (c) Drying (d) Polymerization (e) as-prepared CNT/PPy yarn (f) Washing.

Figure 7.3: **182**

Preparation of PPy-CNT yarn using electropolymerization; (a) pristine CNT yarn and electrochemical cell; (b) photograph of yarn after polymerization showing the coated yarn and a portion of uncoated yarn that was above the electrolyte solution.

Figure 7.4: **183**

SEM micrographs of pristine CNT yarn at (a) low and (b) higher magnification.

Figure 7.5: **185**

SEM micrographs of electrochemically prepared PPy-CNT yarn; surface morphology (a-b) at low and (c) higher magnification and (d-e) cross-section.

Figure 7.6: **186**

SEM micrographs of chemically prepared PPy-CNT yarn; surface morphology (a) at low and (b-d) higher magnification and (e) two-ply PPy-CNT yarn. Areas labelled A and B in (b) highlight less densely coated and more densely coated areas, respectively. The higher magnification micrographs in (c) and (d) were taken from region B.

Figure 7.7:	<b>187</b>
Raman spectra of the pristine MWNT yarn.	
Figure 7.8:	<b>188</b>
Raman spectra of chemically modified the PPy-CNT yarn.	
Figure 7.9:	<b>188</b>
Raman spectra of electrochemically modified the PPy-CNT yarn.	
Figure 7.10:	<b>189</b>
Stress-strain curves obtained from tensile testing of single CNT yarn and chemically prepared single ply PPy-CNT yarn.	
Figure 7.11:	<b>191</b>
Stress-strain curves obtained from tensile testing of chemically and electrochemically prepared two-ply PPy-CNT and pristine CNT yarns.	
Figure 7.12:	<b>192</b>
Cyclic voltammograms of pristine CNT yarn. Potential was scanned between -0.9 and +0.7 V (vs. Ag/Ag <sup>+</sup> ) in 0.10 M Li.TFSI in PC at 100 mVs <sup>-1</sup> .	
Figure 7.13:	<b>193</b>
Cyclic voltammograms of chemically prepared PPy-CNT yarn. Potential was scanned between -0.9 and +0.7 V (vs. Ag/Ag <sup>+</sup> ) in 0.10 M Li.TFSI in PC at 100 mVs <sup>-1</sup> .	
Figure 7.14:	<b>193</b>
Cyclic voltammograms of electrochemically prepared PPy-CNT yarn. Potential was scanned between -0.9 and +0.7 V (vs. Ag/Ag <sup>+</sup> ) in 0.10 M Li.TFSI in PC at 100 mVs <sup>-1</sup> .	
Figure 7.15:	<b>194</b>
Cyclic voltammograms of chemically prepared PPy-CNT yarn. Potential was scanned between -0.9 and +0.7 V (vs. Ag/Ag <sup>+</sup> ) in 1.0 M NaCl aqueous at 100 mVs <sup>-1</sup> .	
Figure 7.16:	<b>194</b>
Cyclic voltammograms of electrochemically prepared PPy-CNT yarn. Potential was scanned between -0.9 and +0.7 V (vs. Ag/Ag <sup>+</sup> ) in 1.0 M NaCl aqueous at 100 mVs <sup>-1</sup> .	

## **Chapter 8**

Figure 8.1:	<b>204</b>
Correlation between electrical conductivity and Young's modulus of as-prepared PPy materials. Filled circles represent fibres based on CNT yarns (a): chemically prepared PPy-CNT yarn (b): electrochemically prepared PPy-CNT yarn. Filled squares are wet-	

spun fibres from soluble PPy-DEHS. Filled diamonds represent the *in situ* reactive spinning using alginate as a host polymer. The points shown as a filled and unfilled triangles represents the electrochemically prepared PPy-DEHS film and PANi-CNT fibre, respectively (added for comparison).

Figure 8.2: **206**

Correlation between conductivity and electroactivity (anodic charge) of as-prepared PPy materials. Refer to Figure 8.1 for an explanation of symbols.

Figure 8.3: **208**

Correlation between electroactivity (anodic charge) and modulus of as-prepared PPy materials. Refer to Figure 8.1 for an explanation of symbols.

## **Tables**

Table 4.1: **83**

Effect of coagulation bath on fibre spinning.

Table 4.2: **88**

Mechanical properties PPy-DEHS and PPy-DEHS/CNT fibres.

Table 4.3: **92**

Effect of temperature, co-solvent and APS oxidant concentration on the properties of the PPy-DEHS product.

Table 4.4: **101**

Ratio of integrated absorption intensities for standard and high molecular weight PPy-DEHS powders.

Table 4.5: **104**

Comparison of elemental analyses for PPy-DEHS samples in their powder form and after fibre spinning.

Table 5.1: **122**

Comparison of the elemental analysis of PPy-DEHS as (i) chemically polymerized powder, (ii) cast film, and (iii) electropolymerized film.

Table 5.2: **126**

Ratio of integrated absorption intensities of Raman bands in PPy samples.

Table 5.3: **128**



Ratio of integrated absorption intensities of chemically and electrochemically prepared PPy-DEHS.

Table 6.1: **165**

Ratio of integrated absorption intensities of Raman bands in PPy-Alg fibre.

Table 6.2: **168**

Effect of the oxidant/dopant on electrical conductivity of as-spun fibres.

## **Schemes**

Scheme 3.1: **59**

Schematic of interaction between DEHS and oxidised polypyrrole

Scheme 6.1: **161**

Schematic of interaction between DEHS and oxidised polypyrrole.

Scheme 6.2: **162**

Chemical structure of Alginate composed of D-mannuronic acid (**M**) and linked L-guluronic acid (**G**) residues.

# Contents

TITLE OF THESIS	I
DEDICATION	II
CERTIFICATION	III
ACKNOWLEDGEMENT	IV
PUBLICATIONS	V
ABSTRACT	VIII
ABBREVIATIONS	X
LIST OF FIGURES	XIII
TABLES AND SCHEME	XXII
CONTENTS	XXIV
<b>CHAPTER ONE</b>	<b>1</b>
<i>Introduction</i>	
1.1 Motivation	2
1.2 Introduction	3
1.2.1 Inherently Conducting Polymers	3
1.2.2 Polyaniline	6
1.2.3 Polypyrrole	9
1.3 Synthesis of Polypyrrole	14
1.3.1 Electrochemical Polymerization of Pyrrole	14
1.3.2 Chemical Polymerization of Pyrrole	14
1.3.2.1 Synthesis of Soluble Polypyrrole	16
1.3.2.1.1 Soluble PPy-DBSA	16
1.3.2.1.2 Soluble PPy with various Functional Dopants	19

1.3.2.1.3 Soluble Polypyrrole with Polymeric Co-dopant	20
1.3.2.1.4 Water Soluble Polypyrrole	21
1.4 Applications of Soluble Polypyrrole	22
1.5 Fibre Spinning	23
1.5.1 Spinning Conducting Polymers	26
1.5.1.1 Spinning of Polyaniline Fibres	26
1.5.1.1.1 Two-Step Spinning of Polyaniline Fibres	26
1.5.1.1.2 One-Step Spinning of Polyaniline Fibres	27
1.6 Aims and Organization of This Thesis	30
1.7 References	32

## **CHAPTER TWO** 38

### *Experimental*

2.1. Introduction	39
2.2. Purification of Polypyrrole Polymers	39
2.2.1. Dialysis	39
2.2.2. Centrifugation	39
2.3 Dynamic Light Scattering (DLS)	40
2.4 Elemental Analyses	44
2.5 Viscometry	44
2.5.1 Intrinsic Viscosity	44
2.5.2 Shear Viscometry	45
2.6 UV-Visible-Near Infrared Spectroscopy	45
2.7 Fourier Transform Infrared (FTIR) Spectroscopy	46
2.8 Raman Spectroscopy	47
2.9 Conductivity Measurements	48
2.10 Dynamic Mechanical Analysis	50
2.10.1 Stress-Strain	50

2.10.2 Viscoelasticity Test	51
2.11 Cyclic Voltammetry	52
2.12 Thermal Analyses	53
2.13 Scanning Electron Microscopy	53
2.14 Transmission Electron Microscopy	54
2.15 Electrochemical Actuation of Polypyrrole	54
2.16 X-ray Diffraction	55
2.17 References	56

## **CHAPTER THREE** 57

### ***Production of Polypyrrole Fibres from Soluble Polypyrrole***

3.1 Introduction	58
3.2 Experimental	59
3.2.1 Materials	59
3.2.2 Characterization Techniques	59
3.2.3 Synthesis of Soluble Polypyrrole	61
3.2.4 Preparation of Fibre Spinning Solution	61
3.2.5 Formation of PPy-DEHS Fibres	62
3.3 Results and Discussion	63
3.3.1 Characterization of Fibre Spinning Solution	63
3.3.1.1 UV-Vis /NIR Spectroscopy	64
3.3.1.2 Dynamic Light Scattering	65
3.3.2 Fibre Spinning	66
3.3.3 Characterization of As-Spun PPy-DEHS Fibre	67
3.3.3.1 Morphology	67
3.3.3.2 Mechanical Properties of PPY-DEHS Fibre	68
3.3.3.3 Electrical and Electrochemical Properties	69
3.4 Conclusions	71

3.5 References	72
----------------	----

<b>CHAPTER FOUR</b>	<b>73</b>
---------------------	-----------

<i>Production of High Performance Polypyrrole Fibres</i>	
--	--

4.1 Introduction	74
------------------	----

4.1.1 PPy-DEHS/CNT Composite Fibre	74
------------------------------------	----

4.2.2 High Molecular Weight Polypyrrole Synthesis	75
---	----

4.2 Experimental	76
------------------	----

4.2.1 Materials	76
-----------------	----

4.1.2 High Performance (High Molecular Weight) PPy-DEHS Fibres	76
--	----

4.2.3 Preparation of Spinning Solutions	77
---	----

(i) PPy-DEHS/CNT Solutions	77
----------------------------	----

(ii) High Molecular Weight PPy-DEHS Solutions	77
---	----

4.2.3 Fibre Spinning	78
----------------------	----

(i) PPy-DEHS/CNT	78
------------------	----

(ii) High Molecular Weight PPy-DEHS	78
-------------------------------------	----

4.3 Results and Discussion	79
----------------------------	----

4.3.1 Characterization of PPy-DEHS/CNT Spinning Solutions	79
---	----

4.3.1.1 TEM micrographs of spinning solution	79
--	----

4.3.1.2 Dynamic Light Scattering	81
----------------------------------	----

4.3.1.3 UV-Vis/NIR Spectra	81
----------------------------	----

4.3.2 Characterization of Spun PPy-DEHS/CNT Fibre	82
---	----

4.3.2.1 Fibre Spinning	83
------------------------	----

4.3.2.2 Morphology	83
--------------------	----

4.3.2.3 Raman Spectra of PPy-DEHS/CNT Fibres	86
--	----

4.3.2.4 Electrical Properties of PPy-DEHS/CNT Fibre	87
---	----

4.3.2.5 Mechanical Properties of PPy-DEHS/CNT Fibre	88
---	----

4.3.2.6 Thermal Properties of PPy-DEHS/CNT Fibre	89
--	----

4.3.3 Production of high Molecular Weight PPy-DEHS Powders and Fibres	90
4.3.3.1 Synthesis of High Molecular Weight PPy-DEHS Powders	90
Influence of [APS oxidant]/ [pyrrole monomer] Ratio	91
Influence of Polymerization Temperature	91
Influence of Ethanol Co-solvent	92
4.3.3.2 Intrinsic Viscosity of PPy-DEHS	95
4.3.3.3 Dynamic Light Scattering	98
4.3.3.4 UV-Vis/NIR Spectra	99
4.3.3.5 FTIR Spectra	100
4.3.3.6 Thermal Properties of PPy-DEHS	102
4.3.3.7 X-ray Diffraction of PPy-DEHS Powders	103
4.3.3.8 Elemental Analyses of PPy-DEHS	104
4.3.4 Production of High Performance PPy-DEHS Fibre	105
4.3.4.1 Viscometry of PPy-DEHS Spinning Solution	105
4.3.4.2 Morphology of Spun PPy-DEHS Fibre	106
4.3.4.3 Mechanical Properties of High Molecular Weight PPy-DEHS Fibre	108
4.3.4.3.1 Drawing of As-Spun PPy Fibre	108
4.3.4.3.2 Mechanical Testing of High Molecular Weight PPy Fibre	110
4.3.4.4 Electrical and Electrochemical Properties of High Molecular Weight PPy Fibre	111
4.4 Conclusions	113
4.4.1 PPy-DEHS/CNT Fibres	113
4.4.2 High Molecular Weight PPy-DEHS Fibres	113
4.5 References	114

<b>CHAPTER FIVE</b>	116
<b><i>Electrochemically Polymerized DEHS Dope Polypyrrole</i></b>	
5.1 Introduction	117
5.2 Experimental	119
5.2.1 Materials	119
5.2.2. Preparation of Electropolymerized PPy-DEHS Film	119
5.2.3 Preparation of Chemically Polymerized PPy-DEHS Films	119
5.3 Characterization of PPy-DEHS Films	119
5.3.1 UV-Vis/NIR Spectroscopy	120
5.3.2 Elemental Analysis of PPy-DEHS Materials	121
5.3.3 Thermal Properties of PPy-DEHS Powder and Films	122
5.3.4 Raman Spectroscopy	123
5.3.5 FT-IR Spectroscopy	126
5.3.6 Morphology of PPy Powder and Films	129
5.3.7 Mechanical Properties of PPy-DEHS Films	131
5.3.8 Electrochemical Properties of PPy-DEHS Materials	133
5.3.9 Electromechanical Actuation of PPy-DEHS Films	136
5.4 Conclusions	139
5.5 References	140
<b>CHAPTER SIX</b>	142
<b><i>Production of Polypyrrole Alginate Fibres</i></b>	
6.1 Introduction	143
6.1.1 Production of PPy/Alg Bicomponent Fibre	144
6.1.2 <i>In Situ</i> Spinning and Polymerization of PPy-Alg Fibre	144
6.1.3 <i>In Situ</i> Spinning and Polymerization of PPy-Alg-CNT Fibre	145
6.2 Experimental	145
6.2.1 Materials	145

6.2.2 Synthesis of Polypyrrole Colloidal Dispersion	145
6.2.3 Preparation of Spinning Solution	146
6.2.3.1 Polypyrrole-Alginate Spinning Solution	146
6.2.3.2 Alginate-Pyrrole Spinning Solution	146
6.2.3.3 Alginate-Pyrrole-CNT Spinning Solution	147
6.2.4.1 PPy/Alg Bicomponent Fibre	147
6.2.4 Fibre Spinning	147
6.2.4.2 PPy-Alg and PPy-Alg-CNT Fibres	148
6.3 Results and Discussion	149
6.3.1 Characterization of PPy-Alg Bicomponent Fibres	149
6.3.1.1 Dynamic Light Scattering	149
6.3.1.2 Viscometry of Spinning Solution	150
6.3.1.3 UV-Vis/NIR Spectra of Spinning Solution	150
6.3.1.4 Production of As-spun PPy-Alg Bicomponent Fibres	151
6.3.1.5 Morphology of As-spun PPy-Alg Bicomponent Fibres	151
6.3.1.6 Mechanical Properties of PPy-Alg Bicomponent Fibre	153
6.3.1.7 Electrical Conductivity of PPy-Alg Bicomponent Fibres	154
6.3.2 Characterization of PPy-Alg and PPy-Alg-CNT Fibres	154
6.3.2.1 Viscometry of Spinning Solution	154
6.3.2.2 Production of As-spun PPy-Alg and PPy-Alg-CNT Fibres	155
6.3.2.3 UV-Vis/NIR Spectra of As-spun PPy-Alg Fibre	155
6.3.2.4 Morphology of As-spun PPy-Alg and PPy-Alg-CNT Fibres	157
6.3.2.5 Raman Spectroscopy of PPy-Alg-CNT Fibres	161
6.3.2.5 Mechanical Properties of As-spun PPy-Alg and PPy-Alg-CNT Fibres	166
6.3.2.9 Electrical and Electrochemical Properties of As-spun Fibres	168
6.4 Conclusions	172
6.4.1 PPy-Alg Bicomponent Fibres	172
6.4.2 PPy-Alg and PPy-Alg-CNT Fibres	172



6.5 References	174
----------------	-----

<b>CHAPTER SEVEN</b>	175
----------------------	-----

<i>Development of Polypyrrole-Carbon Nanotube Yarn</i>	
--	--

7.1 Introduction	176
------------------	-----

7.2.2 Spinning of Carbon Nanotubes Yarn	178
---	-----

7.2.1 Materials	178
-----------------	-----

7.2 Experimental	178
------------------	-----

7.2.3 Preparation of PPy-CNT Yarn	180
-----------------------------------	-----

7.2.4 Electrochemical Preparation of PPy-CNT Yarn	182
---	-----

7.3 Results and Discussion	183
----------------------------	-----

7.3.1 Characterization of PPy-CNT Yarn	183
--	-----

7.3.1.1 Morphology	183
--------------------	-----

7.3.1.2 Raman Spectra of PPy-CNT Yarn	187
---------------------------------------	-----

7.3.1.3 Mechanical Properties of PPy-CNT Yarn	189
---	-----

7.3.1.4 Electrical and Electrochemical Properties of PPy-CNT Yarn	191
---	-----

7.4 Conclusion	195
----------------	-----

7.5 References	196
----------------	-----

<b>CHAPTER EIGHT</b>	197
----------------------	-----

<i>General Conclusions</i>	
----------------------------	--

8.1 Background	198
----------------	-----

8.2 Conclusions from Thesis	199
-----------------------------	-----

8.3 Comparison of Fibre properties	203
------------------------------------	-----

8.4 Fibre Actuators	207
---------------------	-----

8.5 Overall Conclusions and Recommendations for Future Work	208
---	-----

8.6 References	210
----------------	-----